Nuclear Materials and Energy 15 (2018) 208–213

Contents lists available at ScienceDirect

Nuclear Materials and Energy

journal homepage: www.elsevier.com/locate/nme

Microstructure change of duplex stainless steels after thermal aging and electron beam irradiation

Yuta Suzuki[a], Naoyuki Hashimoto[b,*]

[a] Graduate School of Engineering, Hokkaido University, Sapporo 060-8628, Japan
[b] Faculty of Engineering, Hokkaido University, N13W8, Kita-ku, Sapporo 060-8628, Japan

ARTICLE INFO

Keywords:
Spinodal decomposition
Accelerated irradiation
Thermal aging

ABSTRACT

Duplex stainless steel has been used as a structural material for light water reactors. It is well known that the thermal aging during operation causes spinodal decomposition to Cr-rich (α') phase and Fe-rich (α) phase in the ferrite phase, resulting in brittlement. In order to understand the mechanism of this phenomena and the effect of irradiation, a duplex model alloy (Fe-25Cr-10Ni-2.5Mo-1Mn) prepared by arc melting and thermally aged in the appropriate condition was subjected to accelerated irradiation by a multi-beam ultra-high voltage electron microscope and partially an ion accelerator in this study. Spinodal decomposition of Fe and Cr was confirmed in the model alloy aged at 450 °C. In addition, the electron beam irradiation to aged model alloy resulted in the decrease in the amplitude of spinodal decomposition. From this experiment, it was suggested that spinodal decomposition could be suppressed by accelerated irradiation.

1. Introduction

Duplex stainless steel has been used as a structural material for light water reactors due to its strength, irradiation resistance and corrosion resistance. Duplex stainless steel is consisted of ferrite phase and austenite phase. It is well known that thermal aging during operation causes spinodal decomposition to Cr-rich (α') phase and Fe-rich (α) phase in the ferrite phase and G-phase ($M_6Ni_{16}Si_6$, M = Mn, Mo etc.) precipitation, resulting in brittlement [1–5]. MD simulation for neutron-irradiated reactor pressure vessels indicated that the formation of displacement cascade would cause atomic mixing and this disordering could inhibit spinodal decomposition [6]. In addition, the neutron irradiation may also change the location of the phase fields in the phase diagram and effect on the decomposition process [7]. Miller et al. investigated a neutron-irradiated Fe-32Cr by using atom probe field ion microscopy [8], and reported the enhancement of spinodal decomposition. This result is consistent with the neutron irradiation significantly changing the location of the phase field in the phase diagram. Furthermore, it was reported that neutron-irradiated stainless-steel (90% austenite and 10% d-ferrite phases) showed spinodal decomposition in a manner similar to that resulting from thermal aging [9]. In order to clarify the mechanism of this complicated phenomena, it is necessary to carefully investigate the superimposition effect of neutron irradiation and thermal aging, however, it is difficult to perform neutron irradiation and thermal aging simultaneously. One solution would be the simulated irradiation by electron beam and in-situ observation of microstructure change. Nakai and Kinoshita reported the e-irradiation-induced spinodal decomposition in alloys [10], but less in-situ observation studies in Fe-Cr system. In this study, a duplex model alloy was prepared and thermally-aged in some conditions, the electron irradiation was performed by using a multi-beam ultra-high voltage electron microscope in order to clarify the effect of defect flow on spinodal decomposition.

2. Experimental

Material used in this study was a duplex model alloy (Fe-25Cr-10Ni-2.5Mo-1Mn) arc-melted in Ar atmosphere. Table 1 shows the chemical composition of the model alloy. Si was detected by absorptiometry and Cr, Ni, Mn and Mo were detected by ICP emission spectroscopy. Fig. 1 shows a STEM-EDS mapping of the model alloy annealed at 700 °C for 1.5 h. In general, ferrite-forming elements (Cr and Mo) tend to dissolve in the ferrite phase and an austenite-forming element (Ni) does in the austenite phase. The model alloy was thermally aged at 450 °C for 480, 1000, and 3400 h in vacuum. The aging temperature was decided in order to successfully introduce spinodal decomposition in the model alloy. The aged model alloy was gently ground down to 0.15 mm in thick, and punched out to 3 mmφ. This disk was electro-polished by "−5% perchloric acid + acetic acid solution" at room temperature. TEM observation was performed to several samples using a

* Corresponding author.
E-mail address: hasimoto@eng.hokudai.ac.jp (N. Hashimoto).

https://doi.org/10.1016/j.nme.2018.04.013
Received 13 December 2017; Received in revised form 27 April 2018; Accepted 29 April 2018

Table 1
Chemical composition of the model alloy (wt%).

Cr	Ni	Mn	Mo	Si	Fe
24.87	10.07	0.87	2.51	0.01	Bal.

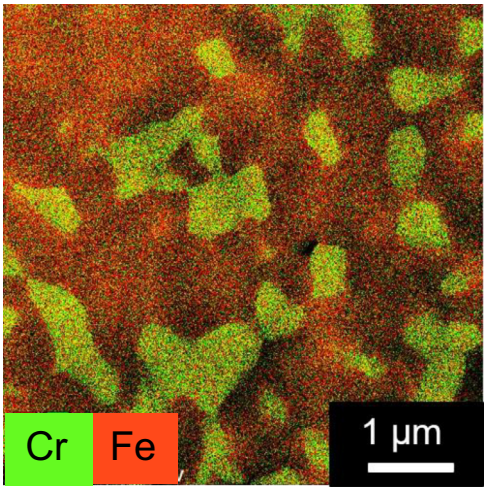

Fig. 1. STEM-EDS mapping of Fe (red) and Cr (green) in the model alloy annealed at 700 °C for 1.5 h. The red area indicates γ-phase (Fe-10 wt%Cr) and the green area does α-phase (Fe-35 wt%Cr). (For interpretation of the references to colour in this figure legend, the reader is referred to the web version of this article.)

Table 2
Electron-irradiation experiment condition.

Dose rate (dpa/s)	1×10^{-4}–1×10^{-3}
Temperature (°C)	250–400
Dose (dpa)	0.1–10

conventional TEM (JEM-2010, JEOL) at accelerating voltage of 200 keV. STEM observation was performed using a Cs-corrected STEM (Titan) at accelerating voltage of 300 keV. In order to eliminate the contamination, Plasma Cleaning was performed prior to STEM observation. Electron irradiation experiment was performed using a multi-beam ultra-high electron microscope (JEM-ARM-1300, JEOL) operated at 1250 keV. The current density of electron beam was measured by Faraday cup inserted into the beam line. The electron beam flux on specimen surface can be controlled by changing beam size and calculated from the electron beam current density. The damage rate (dpa/s) of specimen was calculated from the beam flux and the displacement per atom cross-section of elements. In addition, the electron irradiation temperature was controlled by the heating stage of specimen holder. The increase in temperature of the irradiated area would be at most several percent. The thickness of irradiated area was estimated by using the thickness fringes from the extinction distance of g vector. Table 2 shows the condition of electron irradiation experiment. After the electron irradiation experiment, the number density and size of dislocation loops were analyzed using conventional TEM.

3. Results

3.1. Microstructural evolution in non-aged sample

Fig. 2 shows typical bright field images of ferrite phases in non-aged sample after electron-irradiation to 0.1 dpa and 1 dpa at 300 °C. The imaging condition was $B \sim [001]$, $g = 200$, and $s \sim 0$. Fig. 3 shows the number density and the average diameter of dislocation loops in the electron-irradiated area. The number density and the average size of the irradiation-induced loops were increased as increasing irradiation dose. Fig. 4 shows typical bright field images of ferrite phases in non-aged sample after electron irradiation at 250, 300, 350, and 400 °C. The imaging condition was $B \sim [001]$, $g = 200$, and $s \sim 0$. During electron irradiation, the number density and the average diameter of loops was decreased and increased as increasing irradiation temperature, respectively. Figs. 5 and 6 show the EDS mappings in ferrite phase irradiated to 10 dpa at 250 and 300 °C, respectively. The contrast of spinodal decomposition seemed not to be observed in this irradiation condition, but the enrichment of Fe at dislocation loop was observed instead.

3.2. Microstructural evolution in aged sample

HR-TEM observation was performed to ferrite phase aged at 450 °C for 480 h and 1000 h, the contrast of spinodal decomposition was recognized in all the samples. The contrast of Fe and Cr became higher as increasing thermally aging time. On the other hand, G-phase was not clearly observed in both irradiated and aged model alloy probably due to a lack of Si for G-phase formation. Fig. 7 shows the EDS mapping and the bright field image of ferrite phase aged at 450 °C for 3400 h, and also the line analysis of solute concentration measured by STEM. TEM observation recognized a strong contrast in matrix, however there was no extra spot shown in diffraction pattern. This strong contrast could be due to spinodal decomposition by aging. The mean Cr concentration of the Fe-enriched regions in the ferrite during aging was evaluated by the decomposition fraction (y), which was obtained by Mossbauer spectroscopy [11]. The decomposition fraction (y) is given by $y = (C_t - C_o)/(C_\infty - C_o) \times 100$, where C_o is the mean Cr concentration of the none-aged material, C_t is the mean Cr concentration of the Fe-enriched regions of the material aged for t hours, and C_∞ is the mean Cr

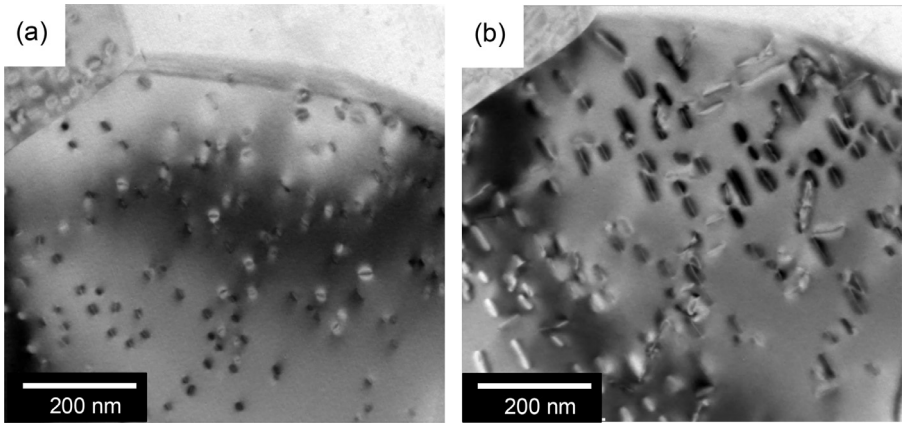

Fig. 2. Typical bright field images of ferrite phases in non-aged sample after electron irradiation to (a) 0.1 and (b) 1 dpa at 300 °C.

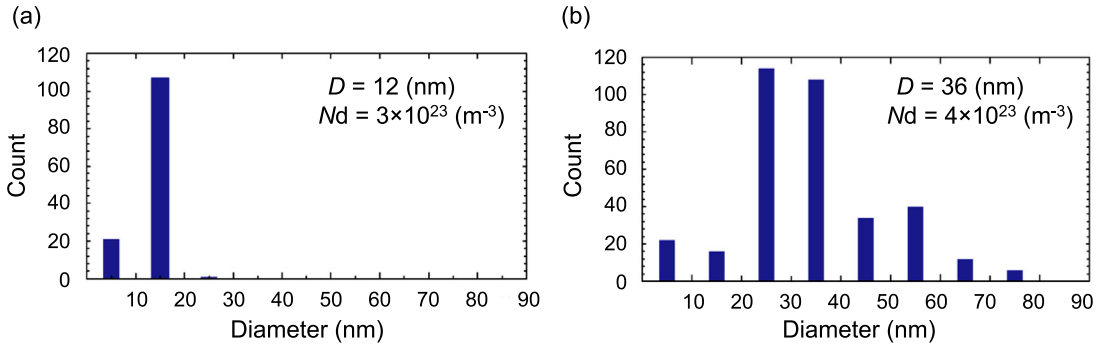

Fig. 3. Number density (*N*d) and average diameter (*D*) of dislocation loops in ferrite phases of non-aged sample after electron irradiation to (a) 0.1 dpa and (b) 1 dpa at 300 ˚C.

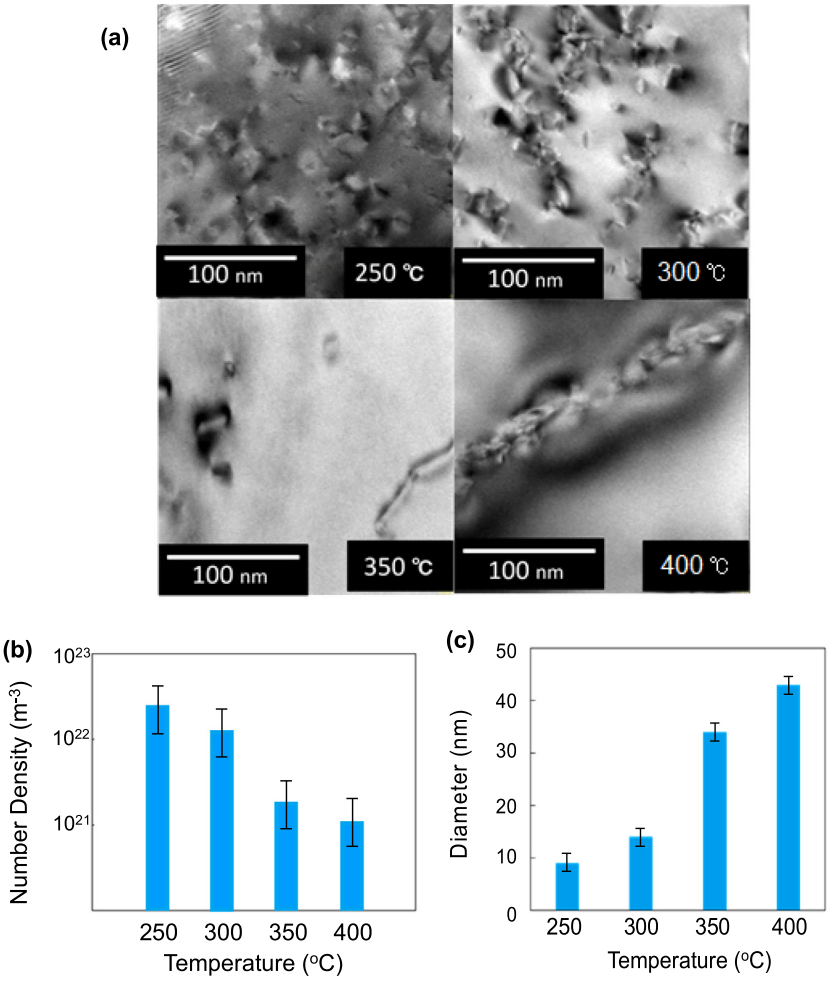

Fig. 4. (a) Typical bright field images of ferrite phases in non-aged sample after electron irradiation to 0.1 dpa at 250, 300, 350 and 400 ˚C. (b) Number density and (c) diameter of loops decrease and increase with the irradiation temperature, respectively.

concentration of the Fe-enriched regions of the final aging condition. The composition fraction of this sample was estimated to be 0.59. The distance of concentration peaks is about 10 nm, which is similar to the width of contrasts taken by TEM. The sample aged at 450 ˚C for 3400 h was electron-irradiated to 10 dpa at 300 ˚C. The damaged microstructure was very complicated, so that it was impossible to estimate the number density of the irradiation-induced loops. Fig. 8 shows the EDS mapping and the line analysis of the ferrite phase which aged 450 ˚C for 3400 h and irradiated to 10 dpa at 300 ˚C. The morphology of spinodal decomposition seemed not to be changed by electron irradiation, but the intensity of contrast was weakened. The decomposition fraction of this electron-irradiated sample was 0.22, which is much less than that of aged sample (0.59).

4. Discussion

Non-aged duplex model alloy (Fe-25Cr-10Ni-2.5Mo-1Mn) was electron-irradiated at 300 ˚C in order to investigate if the spinodal decomposition occurred under accelerated irradiation. The damage rate of electron irradiation in this material was 1×10^{-4} dpa/s, meaning that the irradiation time was about 2.6 h. In this condition, no spinodal decomposition was observed. On the other hand, it was reported that

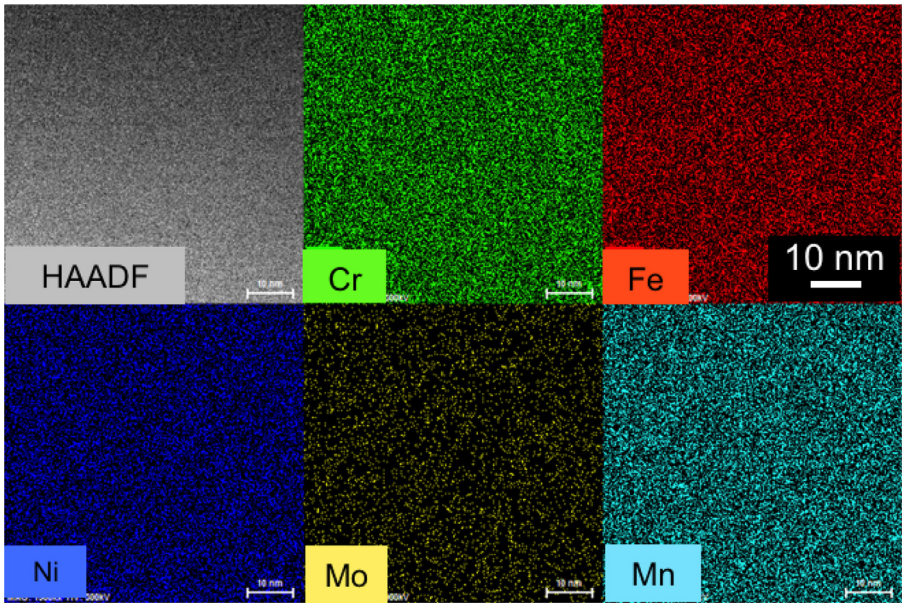

Fig. 5. HAADF image and EDS mapping of ferrite phase in non-aged sample after electron irradiation to 10 dpa at 300 °C.

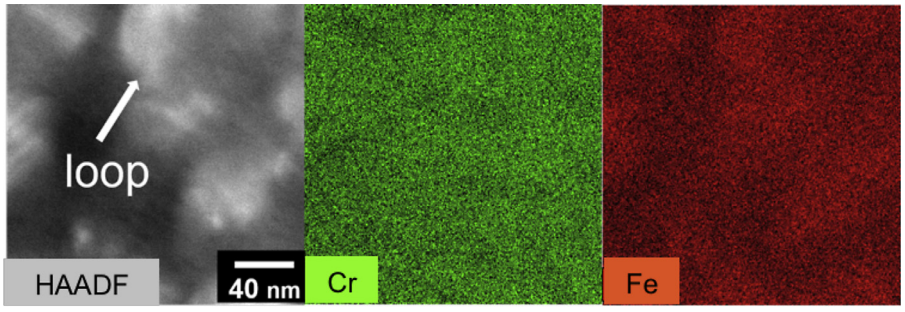

Fig. 6. HAADF image of dislocation loops and EDS mapping of Cr and Fe of ferrite phase in non-aged sample after elctron irradiation to 10 dpa at 250 °C.

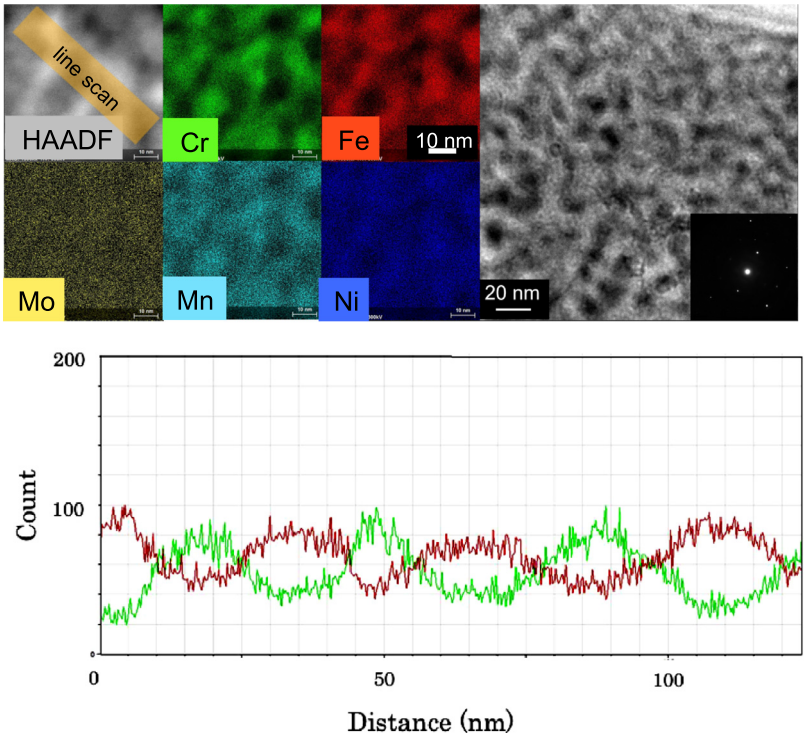

Fig. 7. EDS mapping and the bright field image of ferrite phase aged at 450 °C for 3400 h and the line analysis of solute concentration measured by STEM.

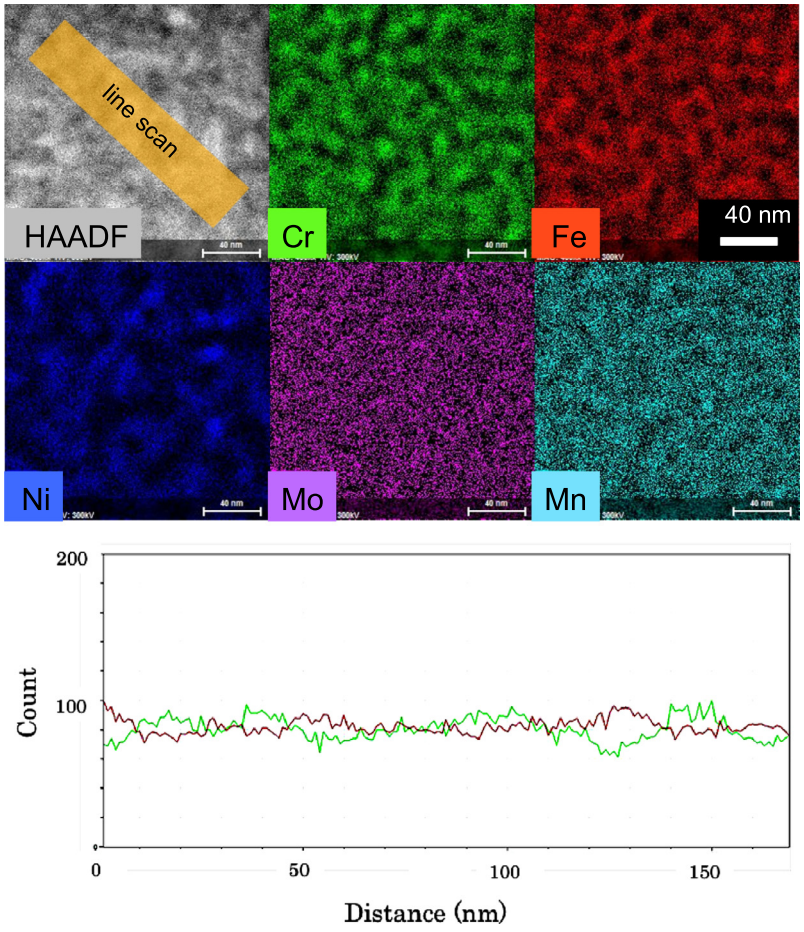

Fig. 8. EDS mapping and the line analysis of solute concentration of ferrite phase aged at 450 °C for 3400 h and irradiated to 10 dpa.

neutron irradiation to Fe-20Cr-10Ni-0.02Mo-1.3Mn at 290 °C resulted in spinodal decomposition [9]. Furthermore, it is also reported that the spinodal decomposition may be accelerated by neutron irradiation [8]. The operation time of this neutron irradiation was about 80 times longer than that in the electron irradiation experiment. In addition, the neutron irradiation normally introduces cascade damage in materials, while the electron irradiation does only primary knock-on atoms (PKAs). In order to investigate the effect of cascade damage on spinodal decomposition, the Fe^{+} ion irradiation experiment was also performed for the non-aged duplex model alloy in the condition same as the electron irradiation, however, any spinodal composition was not observed. Therefore, it is suggested that the spinodal decomposition could hardly occur by accelerated irradiation in this material.

The aged duplex model alloy exhibited spinodal decomposition, and the intensity of recognized contrast in bright field images seemed stronger in the longer aged sample. The electron irradiation to the aged samples resulted in the weaken amplitude of spinodal decomposition. This decrease of intensity has also been reported in the thermally aged duplex stainless steels after ion irradiation [12]. This result could be relating to the non-equilibrium steady state under the accelerated irradiation. Fig. 9 shows Gibbs free energy diagram with a schematic phase diagram. The diagram was calculated by using the software: Pandat, version 9.1. The result of calculation exhibited that the Gibbs free energy at the Cr concentration (0.25) of ferrite phase in the model alloy seemed to be satisfied with the spinodal decomposition condition (indicated in black line). The electron and/or ion irradiation would increase the Gibbs free energy of the ferrite phase, so that the spinodal decomposition could become energetically unstable (indicated in red line). It was reported by Wikes that the phase diagram could be changed by irradiation damage, especially at higher damage rate condition, and furthermore, the ordered structure could be destroyed in the end [13].

With consideration of previous reports and the results of this study, it is suggested that spinodal decomposition in the duplex model alloy would be suppressed by accelerated irradiation. However, the mechanism of spinodal decomposition under irradiation is still unknown, therefore, the well-designed experiment and the detail analysis should be needed.

5. Summary

In order to investigate the mechanism of spinodal decomposition in the duplex model alloy, the accelerated irradiation experiments were performed in non-aged and aged samples in various conditions. The results obtained are summarized as below.

(1) Accelerated irradiation (electron and Fe+ ion) to the non-aged duplex model alloy introduced dislocation loops in matrix, and the number density and the size of dislocation loops was decreased and increased as increasing irradiation temperature, respectively.
(2) The aging in a certain condition resulted in clear spinodal decomposition in the duplex model alloy, while spinodal decomposition was not recognized in non-aged duplex model alloy after accelerated irradiation.
(3) Accelerated irradiation resulted in the decrease in the amplitude of spinodal decomposition, suggesting that spinodal decomposition in the duplex model alloy would be suppressed by accelerated irradiation.

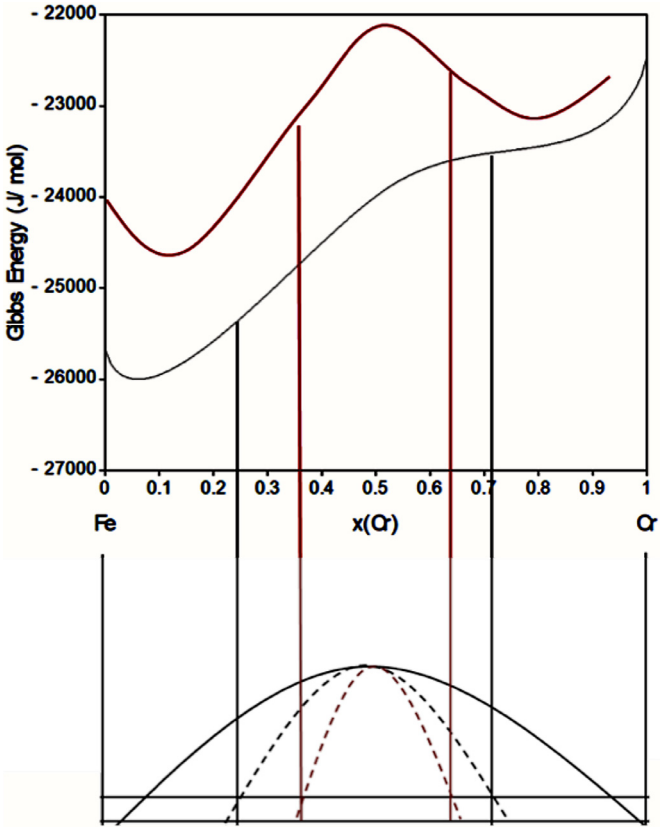

Fig. 9. Gibbs free energy diagram with a schematic phase diagram. Black and red line indicates before and after irradiation, respectively. (For interpretation of the references to colour in this figure legend, the reader is referred to the web version of this article.)

Acknowledgments

The authors wish to thank Dr. Wang for operating TEM and to Mr. Ohkubo and Mr. Tanioka for operating the High Voltage Electron Microscope at Hokkaido University.

References

[1] A. Mateo, L. Llanes, M. Anglada, J. Mater. Sci. (1997) 4533–4540.
[2] O.S. Vargas, E.O. Avila-Davlia, V.M. Lopez-Hirata, N.C. Castro, J.L. Gonzalez-Velazquez, Mater. Sci. Eng. A 527 (2010) 2910–2914.
[3] F. Danoix, P. Auger, D. Blavette, Microsc. Microanal 10 (2004) 349–354.
[4] O.K. Chopra, Semiannial, (1992) Report, NUREG/CR-4744.
[5] K. Fukuya, K. Fujii, H. Nishioka, Y. Kitsunai, J. Nucl. Sci. Tech. 43 (2006) 159.
[6] R.S. Averback, T. Diaz de Ia Rubia, R. Benedek, Nucl. Instrum. Meth. B33 (1988) 693–700.
[7] R.H. Zee, P. Wilkes, Phase Stability During Irradiation, in: J.R. Holland, L.K. Mansur, D.I. Potter (Eds.), The Metallurgical Society of AIME, Warrandale, PA, 1981, p. 295.
[8] M.K. Miller, R.E. Stoller, K.F. Russell, J. Nucl. Mater. 230 (1996) 219–225.
[9] T. Takeuchi, Y. Kakubo, Y. Matsukawa, Y. Nozawa, Y. Nagai, Y. Nishiyama, J. Katsuyama, K. Onizawa, M. Suzuki, J. Nucl. Mater. 443 (2013) 266–273.
[10] K. Nakai, C. Kinoshita, J. Nucl. Mater. 169 (1989) 116–125.
[11] T. Yamada, J. Nucl. Mater. 350 (2006) 47–55.
[12] K. Fujii, K. Fukuya, J. Nucl. Mater. 440 1–3 (2013) 612–616.
[13] P. Wilkes, J. Nucl. Mater. 83 (1979) 166.